Biological, Electronic, NLO, NBO, TDDFT and Vibrational Analysis of 1-benzyl-4-formyl-1H-pyrrole-3-carboxamide

Kumar Pandey, Anoop
Govt. College Bishrampur Surajpur Chhattisgarh, INDIA

Narayan Mishra, Vijay
Sri Ramshwaroop Memorial Institute of Engineering and Management Lucknow, INDIA

Singh, Vijay*[+]
The University of Dodoma, Dodoma, TANZANIA

ABSTRACT: *Biological Electronic, Optical Properties and Vibrational Analysis of 1-benzyl-4-formyl-1H-pyrrole 3carboxamide are studied by using a combination of DFT/B3LYP method and 6-311G (d, p) basis set. Optimized parameters of the title molecule are well-matched with the experiments. The NLO properties of 1-benzyl-4-formyl-1H-pyrrole 3carboxamide have been examined with the help of Polarizability and Hyper-Polarizability. The electronic properties of 1-benzyl-4-formyl-1H-pyrrole 3carboxamide are described with the help of HOMO, LUMO composition. The UV spectra suggest that a strong excitation line occurs at 2.03 eV (160 nm) due to H-2→LUMO (30%). NBO analysis shows that hyper conjugative interaction energy has higher value during LP→ π*, π→ π* transitions. Several biological activities are calculated by PASS software. Docking of the molecule is performed with 5P4Q protein and FF score is -1051.65A.U.*

KEYWORDS: *Vibrational analysis; NBO; NLO; DFT; Electronic properties; PASS.*

INTRODUCTION

Quantum Chemical calculations give important information about molecular geometry, vibrational frequency, electronic properties, UV spectra analysis as well as NLO properties of a molecule. [1-2] Benzyl is the substituent possessing the benzene ring attached to a CH_2 group ($C_6H_5CH_2$-). [3] The position of the first carbon bonded to benzene or another aromatic ring is described as benzyl. The 4-formyl-1H-pyrrole-3 carboxamide is a heterocyclic aromatic organic compound in which three hydrogen of Pyrrole ring (five-membered) replaced by formyl, carboxamide, and Benzyl group. Heterocyclic compounds are those cyclic compounds that contain at least two different elements as 'ring members' atoms. These compounds are organic or inorganic, within the ring structure containing one carbon atom, and one or more atoms of elements other than carbon, such as sulphur, oxygen, nitrogen, etc. Simple N heterocycles have acknowledged significant consideration because of

***** *To whom correspondence should be addressed.*
+ E-mail: drvijay239@gmail.com
1021-9986/2020/1/233-242 10/$/6.00

their important biological properties and their role as pharmacophores. [4.] The introduction of acyl group on nitrogen atom of pyrrole possesses medicinal importance. [5]. In chemistry, formylation is termed as addition of formyl functional group. Formylation has been identified in several critical biological processes [6]. Pyrrole rings have pharmacological as well as biological implications [7]. The derivatives of Pyrroles are very important in drug discovery. [8] These derivatives are used as pharmacological activity such as anti-inflammatory [9], antibacterial [10-13], antioxidant [14] and antitumour agents [15]. Qi-Di Zhong etal. synthesized new pyrrole derivatives 1-benzyl-4-formyl-1H-pyrrole 3carboxamide with good biological activities, and also reported its crystal structure. The present work on 1-benzyl-4-formyl-1H-pyrrole 3carboxamide has been carried out to support and as an extension of the work of Qi-Di *Zhong et al.* [16] In this paper we perform a complete quantum chemical study of 1-benzyl-4-formyl-1H-pyrrole 3carboxamide by using combination DFT/B3LYP method and 6-311G (d, p) basis set. To verify its biological activity several biological activities have been calculated using PASS software and docking is performed by appropriate target.

Computational Methods

Initial geometry of the molecule is modeled with the help of Gauss View 5.0 by using slandered parameters. Geometry optimization is done without any constraint in the potential energy surface. The gradient corrected Density Functional Theory (DFT) with the three-parameter hybrid functional (B3) [17] for the exchange part and the Lee-Yang-Parr (LYP) correlation function [18] has been employed for the computation of molecular structure, vibrational frequencies, HOMO-LUMO, by using GAUSSIAN 09 [19]. Vibrational frequency assignments were made with a high degree of accuracy by combining the results of the GAUSSVIEW'S program [20] with symmetry considerations. In this study, 6-311G(d, p) basis set with d polarization function for heavy atoms and p polarization function for hydrogen atom is used. 6-311G(d, p) basis set gives better description of polar bond in our study. [21-22] Natural bond analysis is calculated by NBO3.0 program package [23].

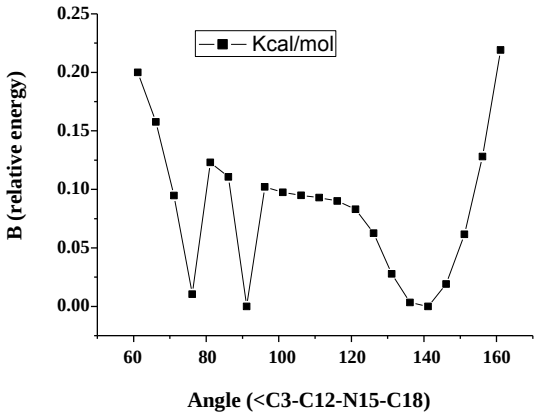

Fig. 1: PES Scan of dihedral angle <3C-12C-15N-18C with 20 step each of 5^0.

RESULTS AND DISCUSSIONS

Optimization

The local minimum energy obtained by structure optimization of the molecule is approximately 716.02957909 A.U. Animated gauss view picture shows that the molecule has no point group symmetry. For optimized parameters bond length is measured in A^0 and bond angle in degrees. To obtain global minima we scan dihedral angle <3C-12C-15N-18C with 20 step each of 5^0 and then plot a graph (Fig. 1) in between relative energy and dihedral angle. From this plot, conformer with dihedral angle <3C-12C-15N-18C = 91.147 ^{0} (shown Fig. 3) has the lowest energy. This conformer has 0.01041 kcal/mol lower energy than next stable conformer with<3C-12C-15N-18C = 76.147^0. For sake of simplicity we have considered the most stable conformer for our study. In the molecule there are two rings namely pyrrole and benzyl rings, nearly perpendicular, are connected with methyl group. The calculated geometry parameter are compare with experimental data in Supplementary Table 1. The calculated (C-N) bond length, lies in between 1.3976Å- 1.3488Å, is in agreement with experimental results [16](1.37Å -1.36Å) while calculated (N-H) bond length lies in between 0.9973Å- 0.9937Å, which matches with experimental value (1 Å). The C-O bond length is found to be 1.37 Å however experimental value is 1.29 Å. In Fig. 2 we plot a graph between experimental and calculated bond length of the molecule. Graph shows linear relation and after linear correlation between experimental bond lengths with calculated bond length by DFT method we find correlation equation

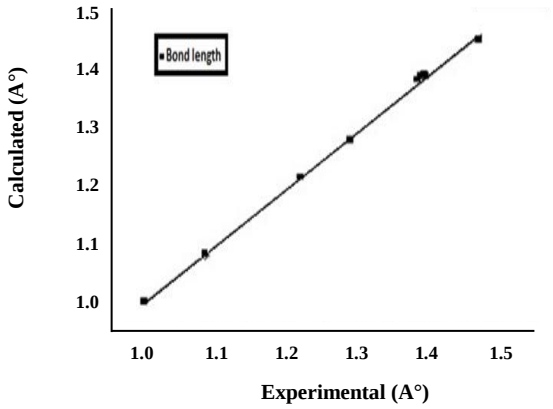

Fig. 2: Comparison between experimental and theoretical bond length.

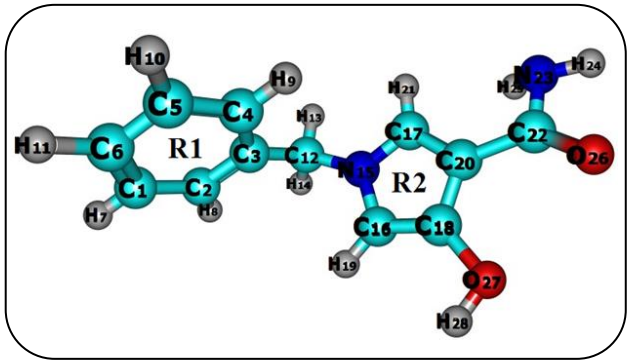

Fig. 3: Model molecular structure of 1-benzyl-4-formyl-1H-pyrrole-3carboxamide.

Calculated = 0.98062 experimental + 0.01911 with correlation factor R^2=0.99861.

The correlation factor >0.99 shows that the DFT can reproduce experimental result well. The angular changes in benzene ring geometry have proved to be a sensitive indicator of the interaction between the substituent and the attached ring. The (C-N-C) bond angle varies from 124.82^0- 109.40^0 while (C-N-H) varies between 181.07^0- 123.24^0.

Polarizability, Hyper polarizability and thermodynamic properties

The Dipole moment (μ), polarizability <α> and total first static hyper polarizability β are used to determine NLO property of title molecule.[24-25] These parameter are calculated by using combination of DFT/B3LYP method and 6-311G(d, p) basis set (supplementary Table-2). First order hyperpolarizability is a third rank tensor of 3×3×3 matrix. By using Kleinman symmetry, consideration 27 components of the 3-D matrix can be reduced to 10 components.[26] Polarizability and hyperpolarizability belongs to first and higher order derivatives of the electron density which is helpful to determine shape and interaction characteristics of chemical bond in molecule. These parameter can be expressed in terms of *x, y, z* components and are given by following equations 1, 2,3

$$\mu = \left(\mu_X^2 + \mu_Y^2 + \mu_Z^2\right)^{1/2} \quad (1)$$

$$< \alpha >= 1/3\left[\alpha_{xx} + \alpha_{yy} + \alpha_{zz}\right] \quad (2)$$

$$\beta_{Total} = \left(\beta_x^2 + \beta_y^2 + \beta_z^2\right)^{1/2} = \left[\left(\beta_{xxx} + \beta_{xyy} + \beta_{xzz}\right)^2 + \left(\beta_{yyy} + \beta_{yxx} + \beta_{yzz}\right)^2 + \left(\beta_{zzz} + \beta_{zxx} + \beta_{zyy}\right)^2\right]^{1/2} \quad (3)$$

The β components of Gaussian output are reported in atomic units.

Where (1 a.u. = $8.3693X10^{-33}$ e.s.u.).

For 1-benzyl-4-formyl-1H-pyrrole-3carboxamide molecule, calculated dipole moment value is 4.2863 Debye which is greater than dipole moment of water (2.16 Debye), is attributed to electron withdrawing group –COONH2- and –OH- group present on hetro-cyclic ring. From supplementary Table 2 we see higher contribution of axial component in polarizibility shows that molecule is elongated more towards axial direction. In hyperpolarizibilty $\beta_{xxx,}$ β_{xzz} component having larger contribution shows that a larger electron density along bond along X direction and XZ plane. This shows that X axis and XZ plane are more optical active directions. The calculated values for the total intrinsic hyperpolarizability β_{TOTAL} and the component of the hyperpolarizability ($\vec{\beta}$) are given in supplementary Table 2. The calculated value β_{TOTAL} of title molecule ($0.9339x10^{-30}$ e.s.u.) is nearly five times greater than hyperpolarizibilty of urea ($0.19347x10^{-30}$e.s.u.) so title molecule use as NLO active molecule

Thermodynamical Properties

Thermodynamic properties like entropy, enthalpy and heat capacity at various temperatures (100-400 K) have been calculated (Fig. 4) by DFT/6-311G(d, p) method from the theoretical vibration analysis. These parameters increase with temperature. The graphs between

Table 1: The observed UV-vis spectra are calculated by TD-DFT method at B3LYP/6-311 G (d, p) level.

Excitation energy (eV)	wavelength (nm)		Oscillator strength	Orbital transition
	Calculated	Assignment		
4.12	250.62	n→π*	0.0008	H-4->L+1 (26%)
2.03	160.20	π→ π*	0.2305	H-2->LUMO (30%)

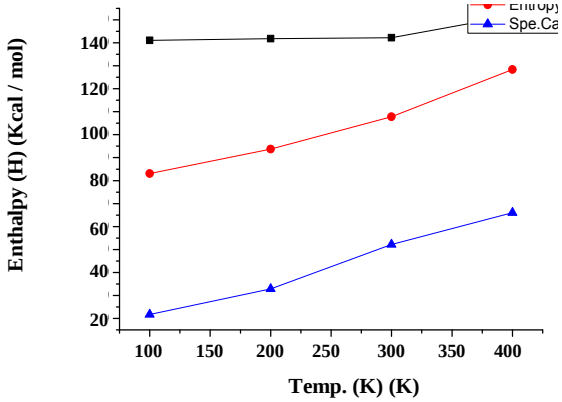

Fig. 4: Graph plotted between entropy enthalpy Heat capacity V/S Temperature (K) calculated by DFT/6-311G (d, p) method.

temperature-entropy and enthalpy -heat capacity are plotted and fitted in quadratic formula of order two. The fitting factors for these calculated thermodynamic properties are 0.97519 (for C), 0.99873 (S) and 0.9899 (H), respectively, while the second order quadratic fitting equations are as follows

H^0_m=147.1585-0.07799T+.000221T^2 (R^2= 0.9899)

$C^0_{p.m}$=8.503+0.11861T+0.000067T^2 (R^2=0.97519)

S^0_m= 78.14075+0.02638T+0.000247T^2 (R^2=0.99873)

These quadratic equations give significant information about thermochemical field to calculate thermodynamic energy.

Electronic Properties and UV Spectra

The interaction of the molecule with other chemical system is resolute by frontier orbitals, FHOMO and FLUMO which can be verified by experimental data. The frontier orbital gap is equal to HOMO-LUMO gap which helps to determine the kinetic stability and chemical reactivity of the molecule. The molecule is termed as soft molecule when it becomes more polarizable, high chemically reactive, low kinetically stabile and have small frontier orbital gap. [27] The frontier orbital gape calculated for given molecule is 6.20 eV, shows molecule is less chemically active. The contour plots of HOMO, LUMO orbital and MESP of the molecule are shown in Fig. 4. In this plot HOMO, which primarily acts as donor is distributed over R_2 ring of the molecule while LUMO behaves as acceptor distributed over benzene ring. The transition from HOMO→LUMO shows that charge is transferred from ring R_2 to benzene ring.

The MESP plot gives valuable information about reactive site to positive, negative, and neutral electrostatic potential region in terms of color coding e.g red as electro negative, blue as electro positive and yellow as neutral site[28-30]. MESP of the molecule visibly suggests that the major electronegative potential region (shaded with Red colour) O_{27}, O_{26} atoms of –CONH2- group and most electropositive region C_{22} (shaded with blue colour).

UV spectra TDDFT analysis

Time dependent density theory is important tool for the study of the nature of transition of electron in title compound. After optimization by using combination of DFT/B3LYP method and 6-311G (d, p) basis set, we have used TD-DFT calculation with same level theory to find energy of various transition state. The calculated electronic transition energies (Table 1) at 4.12 eV (250.62 nm) and 2.0 3eV (160.20 nm) mainly originate due to H-4→L+1(26%), H-2→LUMO(30%) transitions respectively. The plot and transition of HOMO-4(MO=53), H-2(MO=55), LUMO (MO=58) LUMO+1(MO=59) of the molecule is shown in Fig. 6. HOMO-2 is localized over Benzene ring (as HOMO) however HOMO-4 is localized over –$CONH_2$-group. The LUMO and LUMO+1 are nearly localized over whole molecule. So the transitions from H-4→L+1 and H-2→LUMO show that charge transfer from benzene and –$CONH_2$- group to R_2 ring. A graph is plotted between wavenumber and oscillatory strength and shown in Fig. 5. On the basis of the calculated molecular orbital coefficients analyses electronic transition are assigned to n→π* and π→π* respectively.

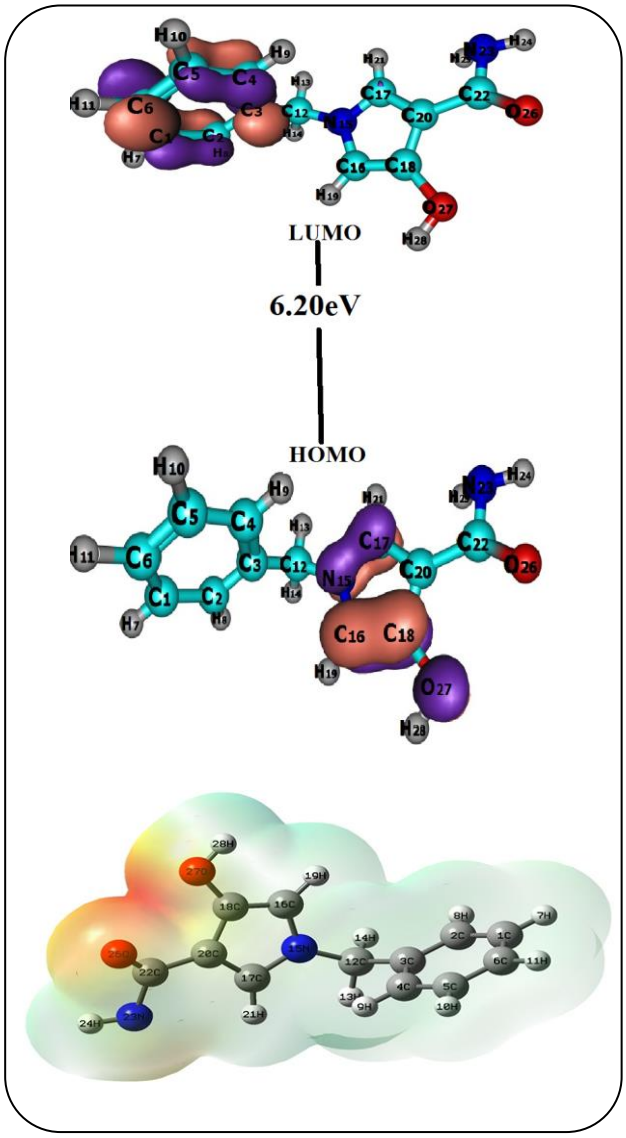

Fig. 4: HOMO - LUMO MESP pictures of 1-benzyl-4-formyl-1H-pyrrole-3carboxamide

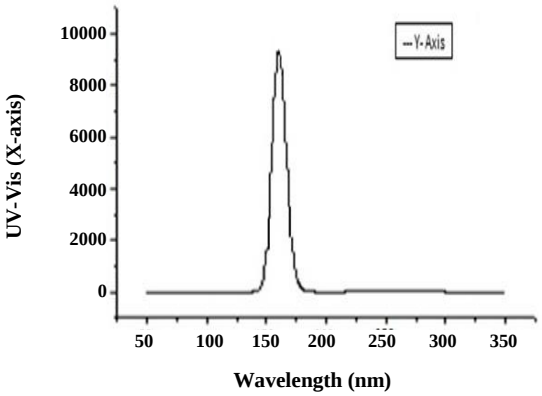

Fig. 5: Calculated UV spectra of Title molecule using combination of DFT/B3LYP method and 6-311G(d,p) basis set.

Assignments of Fundamentals

In 1-benzyl-4-formyl-1H-pyrrole-3-carboxamide has 28 atoms 78 normal modes of vibration. The assignments of the calculated wave numbers are based on animated view of normal mode and listed in supplementary Table 3. The calculated frequencies are typically higher than the experimental one due to combination of electron correlation and anharmonicity. [31-32] Due to this reason thr theoretical frequency is scaled. Vibrational frequencies is scaled by the factor of 0.96 [33]. Some important modes of vibrations are discussed here.

Vibrational modes discription

Ring vibration

The presence of C–H stretching vibrations in the region 2800–3100 cm^{-1}, which is the characteristic region for identification of the C–H group.[33] In the molecule the C-H functional group is present at a number of positions. Three medium intense polarized peaks with polarization vectors directed along ring R_1 appear at 3231 cm^{-1}, 3240 cm^{-1} and 3251 cm^{-1} due to ν(C–H) R1. Two medium intense polarized peaks lying on lower side of spectral region due to β (C-H) R_1 and γ (C-H) R_1 are at 1562 cm^{-1} ,778 cm^{-1} respectively. An intense and a medium intense peaks occur due to mixing of ν(C=C) R_1, β (C-H)R_1 corresponding to 1743 cm^{-1} and 1562 cm^{-1} respectively. A very intense peak occurs due to mixing of in plane O_{27}-H_{28} bending C_{16}-N_{15} stretching in ring R_2 is at 1470 cm^{-1}. The μ(C_{16}-N_{15}) appears as a prominent mode in the FT-IR spectra at 1686 cm^{-1}. Three back to back sharp peak appears due to stretching of C_{16}-N_{15} bond in ring R_2 appears at 1472 cm^{-1}1500 cm^{-1} 1529 cm^{-1} . A very weak intense peak appears at 1115 cm^{-1} due to in plane bending C_{16}-N_{15} -C_{17} in ring R_2 however at lower range of spectra two intense peak appears due to γ (C_{16}-N_{15} -C_{17})R_2 appears at 928 cm^{-1} and 684 cm^{-1} respectively.

-$CONH_2$-group vibration

The –NH_2 and –C=O functional groups are noteworthy elements of the molecule and vibrations corresponding to these groups are present in a number of modes. The N-H stretching vibration generally obtained in the region of 3500-3000 cm^{-1} [34]. In this study at higher frequency region two intense modes due to antisymmetric and symmetric stretching of NH_2 in –$CONH_2$

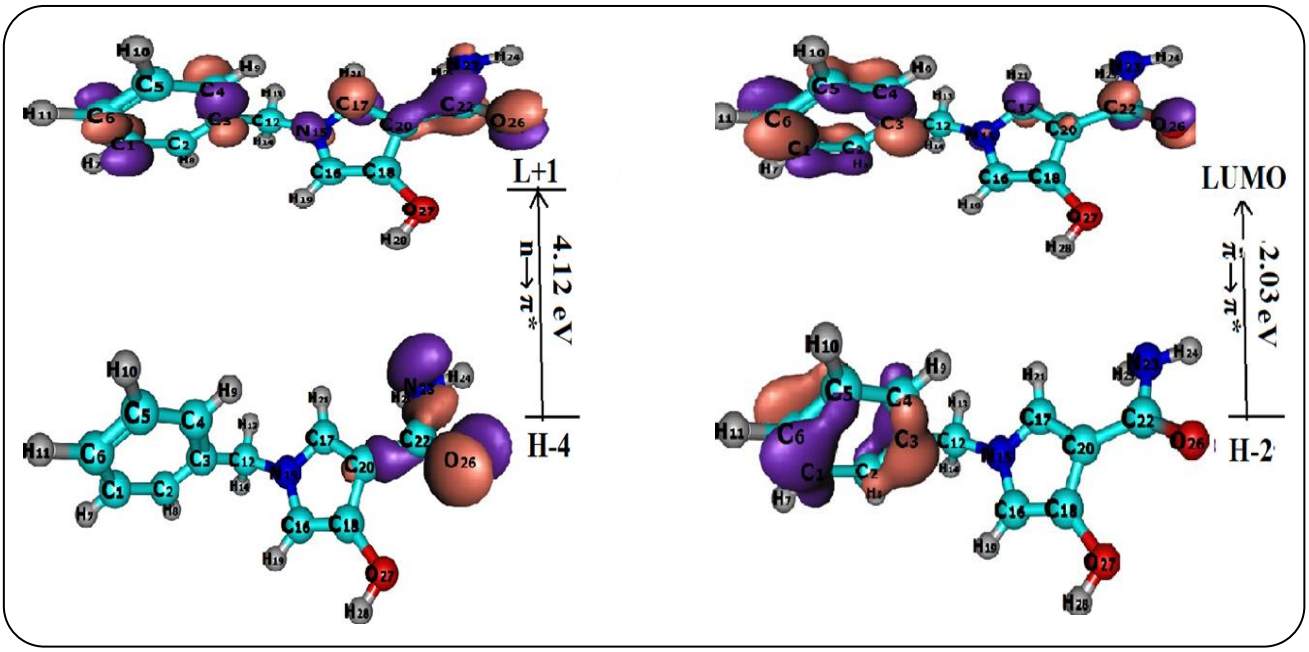

Fig. 6: Electronic Transition of TD-DFT of title molecule by DFT/B3LYP method.

functional group occur at 3637 cm^{-1},3554 cm^{-1}. At lower region frequency two scissoring S(H_{24}-N_{23}-H_{25}) of –$CONH_2$ group are 1682 cm^{-1} and 1145 cm^{-1} and wagging modes ω(H_{24}-N_{23}-H_{25}) R_2 obtained are 1184 cm^{-1}, 1226 cm^{-1}, 856 cm^{-1} and 611 cm^{-1}. The C=O stretching band having high intensity is obtained in the region 1800 cm^{-1}-1650 cm^{-1} [35.], however their exact position is governed by the inter and intra molecular hydrogen bonding, electronic and mass effects of adjacent substituents and conjugations [36-37]. The C-O stretching vibrations intensity increases the probability of formation of hydrogen bonds. The C=O bond is produced by p_π - p_π between carbon and oxygen atoms. In C=O bond bonding electron are not equally distributed but shifted towards oxygen because oxygen is more electronegative than carbon and lone pair electron of oxygen decides nature of the C=O group. In this study a very intense polarized band with polarization vector directed along the plane of adjacent ring occurs at 1785 cm^{-1} due to μ(C_{22}-O_{26}) R_2. In this stretching mode both carbon and oxygen vibrate with equal intensity. Some bending modes due to C_{22}-O_{26}in plane bending modes appears lower side of IR spectra with low intensity e.g. 627 cm^{-1}.

Other Modes of Vibration

Pulay *et al* [38] recommended the vibratuinal frequencies on the basis of *internal* coordinate system. NH_2 and CH_2 group connect with six types of vibrational frequencies namely: two stretching modes symmetric, asymmetric and rest four bending modes e.g., scissoring, rocking, wagging and twisting. In which two scissoring and rocking deformations belong to polarized in–plane vibration however wagging as well as twisting deformations belong to depolarized out–of–plane vibration.

In calculated spectra one low intense polarized peak with polarization vector is directed along C_{17}-N_{15} at 3140 cm^{-1} due to μ_{as}(H_{14}-C_{12}-H_{13}) adj R_1 and a medium intense peak occurs at 3097 cm^{-1} due to symmetric μ_s(H_{14}-C_{12}-H_{13}) stretching vibration. . On the lower side of spectra, two intense peaks due to scissoring modes of vibration, occur at 1612 cm^{-1} and 1460 cm^{-1}. A very intense polarized peak occurs at 1472 cm^{-1} with polarization vector directed along bond C_{17}-H_{21} due to S(H_{14}-C_{12}-H_{13})adjR_2.. At higher frequency region an intense polarized peak at 3760 cm^{-1} with polarization vector directed along N_{15}-C_{16} due to μ (O_{27}-H_{28}) R_2 occurs. From lower side of IR spectra two intense peaks occur at 709 cm^{-1},713 cm^{-1} due γ (O_{27}-H_{28}) R_2. The O-H group present in our molecule is expected to be most sensitive which shows noticeable shifts in the spectra of the hydrogen-bonded species.

NBO analysis

Natural bond orbital analysis is used to study interaction among the bond and charge transfer or

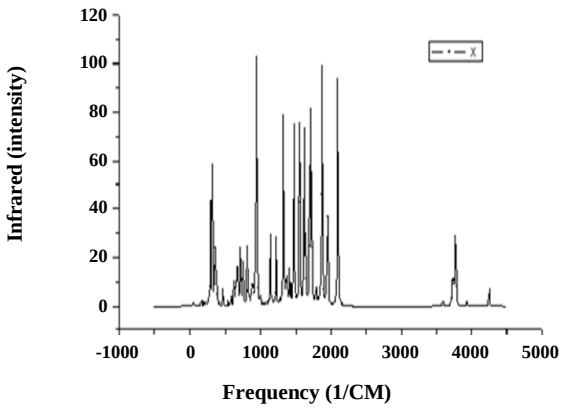

Fig. 7: Calculated IR spectra of Title molecule using combination of DFT/B3LYP method and 6-311G(d, p) basis set.

conjugative interactions in a molecular system. NBO analysis provides information about how electron density gets transferred from the bonding orbitals to the antibonding orbitals [39]. The strength of these interactions depends on the value of the second order energy of interaction between the donor and acceptor orbitals. The interaction between electron donors and electron acceptors is intense If the value of $E^{(2)}$ is high. The second order energy lowering is calculated by using each donor NBO(*i*) and acceptor NBO(*j*) and the strength of delocalization interaction [40]

$$E^{(2)} = -q_i \frac{F_{ij}}{\varepsilon_j - \varepsilon_i}$$

Several significant interactions are listed for the study molecule in Supplementary Table 4. From this table this is clear that σ electron density (1.976e - 1.983e) shows higher value than π electron density (1.862e -1.665e). In this molecule mainly σ → σ* π→ σ*,π→π* ,LP→π*/ σ* interactions occurs between bonding antibonding orbitals i.e. The σ → σ * interactions between bonding and antibonding orbitals are found to be σ (C23-C25)→σ* (C22-O26) and σ (C16-C18)→σ* (C18-C21), having $E^{(2)}$ values of 10.04 kcal/mol and 4.15 kcal/mol respectively. The π→ σ * interactions between bonding and antibonding orbitals which stabilized molecule is found to be π (C2-C3)→σ*(C4-C5) with $E^{(2)}$ 45.21 kcal/mol. The π→ π* interactions between bonding and antibonding orbitals are π (C1-C6) →π* (C2-C3), π (C1-C6)→π* (C4-C5),π (C4-C5) → π* (C2-C3), π (C4-C5) → π* (C1-C6), having $E^{(2)}$ values 46.69 kcal/mol, 46.75 kcal/mol, 48.01 kcal/mol and 45.21 kcal/mol respectively. The strongest interaction LP→ π*/ σ* involving lone pairs and nearly vacant antibonding orbitals such as LP(1) N15→π* (C16-C18)and LP(1) N22→π* (C17-C20) and LP(2)O26→σ* (C22-N23) have high $E^{(2)}$ values of 67.11 kcal/mol 72.42 kcal/mol and 24.69 kcal/mol respectively. These interactions contribute the greatest role to stabilizing the molecule.

Biological activity and docking

PASS [41] predicts Methylenetetrahydrofolate reductase to be inhibitor (0.7610) and having Antiallergic biological activity (0.7180), which is based on the structure activity relationships with Pa > 0.70. In methyl cycle Methylene tetrahydrofolate, reductase is the rate-limiting enzyme .The molecule under study inhibits this enzyme and prevent the human body from Alzheimer, other forms of dementia, colon cancer and acute leukemia disease. The molecule shows better activity against allergic diseases which are caused by hypersensitivity of the immune system typically harmless substances in the environment [42]. Swiss dock [43] is online webserver, which predicts suitable binding protein for the molecule is 5P4Q [44]. The structure 5P4Q has in total one chain with sequence from Cryphonectria parasite. The Cryphonectria parasitica is fungus belonging to Ascomycota taxon pathogen. It is the main cause of chestnut disease, a shocking disease of the American chestnut trees. [45]

After predicting suitable protein we perform docking of the molecule with the trial protein 5P4Q by Swiss Dock web server. All the probable conformers of the ligand and their corresponding energy values are resolute and best binding modes are ranked allowing to the full fitness (FF). This docking process is not covered on specific region of the chosen protein but blind follows whole region of chosen protein. The highest negative values of full fitness score shows best binding site between protein and the taken molecule. The full fitness score obtained in docking is -1051.65 A.U. Docking between title molecule and 5P4Q protein is shown in Fig. 8 using UCSF chimera software. The binding sites between title molecule and 5P4Q protein are H9and LIG (residue) and distance between H9-LIG is 2.169A^0. . FF score and docking between title molecule and 5P4Q protein shows

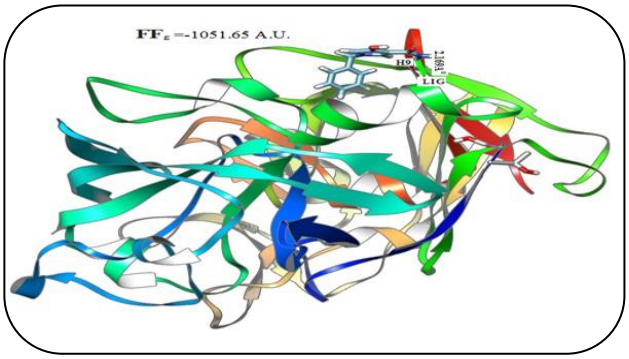

Fig. 8: Docking of Title molecule with 5P4Q protein predicated by Swiss Dock wave server.

that the molecule can be useful to stop fungus related dieseses. This study gives a pathway for drug researcher to design new drugs for fungus related diseases.

CONCLUSIONS

In this paper we calculate geometric parameters, vibrational frequencies, electronic and the non-linear optical properties of title molecule using combination of DFT/B3LYP method and 6-311G (d, p) basis set. Optimized geometry clearly shows that the molecule is non-planar. Correlation factor > 0.99 between calculated and experimental value shows that they are well matched with each other. Non-linear optical behavior of the molecule shows that title molecule is optically active along the plane of the molecule. The molecular electrostatic potential contours and surfaces show that electron density transfer to benzene ring. NBO analysis shows that strongest interaction between bonding and antibonding orbitals is LP (1) N22 $\rightarrow\pi^*$ (C17-C20) with $E^{(2)}$ values 72.42 kcal/mol. The molecule shows better activity against allergic diseases.

Received : Aug. 7, 2018 ; Accepted : Nov. 5, 2018

REFERENCES

[1] Misra N., Prasad O., Sinha L. Pandey A., Molecular Structure and Vibrational Spectra of 2-Formyl Benzonitrile by Density Functional Theory and *ab Initio* Hartree–Fock Calculations, *Journal of Molecular Structure: Theochem*, **822**: 45-47 (2007).

[2] Kumar A., Rawat P., Baboo V., Verma Di., Singh R.N., Saxena D., Gauniyal H.M., Pandey A. K. Pal H., A Combined Experimental and Quantum Chemical Studies on Molecular Structure, Spectral Properties, Intra and Intermolecular Interactions and First Hyperpolarizability of 4-(benzyloxy)benzaldehyde Thiosemicarbazone and Its Dimer, *Journal of Molecular Structure*, **1034**: 374-385 (2013).

[3] Carey F.A., Sundberg R.J., "Advanced Organic Chemistry, Part A: Structure and Mechanisms", 5th ed, Springer, New York, P. 806–808, 312–313 (2008).

[4] Hartner Jr F., Katritzky A., Rees C., Scriven E., "Comprehensive Heterocyclic Chemistry II", ed. I. Shinkai, Pergamon, Oxford, 3, p. 4 (1996)

[5] Bhardwaj V., Gumber D. Abbot V. Dhiman S. Sharma P., Pyrrole: A Resourceful Small Molecule in Key Medicinal Hetero-Aromatics, *RSC Adv.*, **5**: 15233-15266 (2015).

[6] Adams J.M. and Capecchi M.R.., N-Formylmethionyl-sRNA as the Initiator of Protein Synthesis, *PNAS*, **55**(1)**:**147–155 (1966).

[7] Bellina F., Rossi R., Synthesis and Biological Activity of Pyrrole, Pyrroline and Pyrrolidine Derivatives with Two Aryl Groups on Adjacent Positions, *Tetrahedron*, **62**: 7213-7256 (2006).

[8] Toja E., Depaoli A., Tuan G., Kettenring J., *Synthesis*, 272-274 (1987).

[9] Chidananda N., Poojary B., Sumangala V., Kumari N. S., Shetty P., Arulmoli T., Facile Synthesis, Characterization and Pharmacological Activities of 3,6-Disubstituted 1,2,4-triazolo[3,4-b][1,3,4] thiadiazoles and 5,6-dihydro-3,6-Disubstituted-1,2,4-triazolo[3,4-b][1,3,4]thiadiazoles, *Eur. J. Med. Chem.*, **51**: 124–136 (2012).

[10] Eweiss N.F., Bahajaj A.A., Synthesis of Heterocycles. Part VII Synthesis and Antimicrobial Activity of Some 7*H*-*s*-triazolo[3,4-*b*][1,3,4] Thiadiazine and *s*-triazolo[3,4-*b*][1,3,4]thiadiazole Derivatives, *J. Heterocycl. Chem.*, **24**: 1173–1181 (1987).

[11] Kotaiah Y., Nagaraju K., Harikrishna N., Rao C. V., Yamini L., Vijjulatha M., Synthesis, Docking and Evaluation of Antioxidant and Antimicrobial Activities of novel 1,2,4-triazolo[3,4-b][1,3,4]thiadiazol-6-yl)selenopheno[2,3-d]pyrimidines, *Eur. J. Med. Chem.*, **75**: 195–202 (2014).

[12] Swamy S.N., Basappa, Priya B.S., Prabhuswamy B., Doreswamy B.H., Shahidhara J.S., Rangappa K. S., Synthesis of Pharmaceutically Important Condensed Heterocyclic 4,6-disubstituted-1,2,4-triazolo-1,3,4-Thiadiazole Derivatives as Antimicrobials, *Eur. J. Med. Chem.*, **41**:531–538 (2006).

[13] Mathew V., Keshavayya J., Vaidya V.P., Heterocyclic System Containing Bridgehead Nitrogen Atom: Synthesis and Pharmacological Activities of some Substituted 1,2,4-triazolo[3,4-b]-1,3,4-thiadiazoles, *Eur. J. Med. Chem.*, **41**: 1048–1058 (2006).

[14] Demir A.S., Akhmedov I.M., Sesenoglu O., Synthesis of 1,2,3,5-tetrasubstituted Pyrrole Derivatives from 2-(2-bromoallyl)-1,3-dicarbonyl Compounds, *Tetrahedron*, **58**: 9793-9799 (2002).

[15] Meshram H.M., Prasad B.R.V, Kumar D.A., A Green Approach for Efficient Synthesis of N-Substituted Pyrroles in Ionic Liquid under Microwave Irradiation, *Tetrahedron Lett.*, **51**: 3477- 3480 (2010).

[16] Zhong Q.D., Hu S., Yan H., Crystal Structure of 1-benzyl-4-formyl-1*H*-pyrrole-3-carboxamide, *Acta Cryst. E*, **72**: 133–135 (2016).

[17] Becke A.D., Density-Functional Thermochemistry. III. The Role of Exact Exchange, *J. Chem. Phys.*, **98**: 5648–5652 (1993).

[18] Lee C.T., Yang W.T., Parr R.G.B., Development of the Colle-Salvetti Correlation-Energy Formula Into a Functional of the Electron Density, *Phys. Rev. B*, **37**: 785–789 (1988).

[19] Frisch M.J., Trucks G.W,. Schlegel H.B. et al., Gaussian 09, Gaussian, Pittsburgh, Pa, USA, (2009).

[20] Frisch A., Nelson A. B., Holder A. J., Gauss View, Gauss, Pittsburgh, Pa, USA, 2000. Pipek J.and Mezey P.Z., A Fast Intrinsic Localization Procedure Applicable for *ab Initio* and Semiempirical Linear Combination of Atomic Orbital Wave Functions, *J. Chem. Phys.*, **90**: 4916- (1989).

[21] Petersson D.A., Allaham M.A., A Complete Basis Set Model Chemistry. II. Open-Shell Systems and the Total Energies of the First-Row Atoms, *J. Chem. Phys.*, **94**:6081–6090 (1991).

[22] Petersson G.A., Bennett A., Tensfeldt T.G., Allaham M.A., Mantzaris W.A.J., Petersson G.A., Bennett A., Tensfeldt T.G., Al-Laham M.A., Shirley W.A., A Complete Basis Set Model Chemistry. I. The Total Energies of Closed-Shell Atoms and Hydrides of the First-Row Elements, *J. Chem. Phys.*, **89**: 2193–2218 (1998).

[23] Glendening E.D., Landis C.R., Weinhold F., Natural Bond Orbital Methods, *Comput. Mol. Sci.*, **2**: 1-42 (2011).

[24] Parr R.G., Yang W., "Density-Functional Theory of Atom und Molecules", Oxford University Press, Oxford, (1989).

[25] Becke A. D., A New Mixing of Hartree–Fock and Local Density-Functional Theories, *J. Chem. Phys.*, **98**: 1372-1377 (1993).

[26] Kleinmann D.A., Nonlinear Dielectric Polarization in Optical Media, *Phys. Rev.*, **126**: 1977-1979 (1962).

[27] Fleming I., "Frontier Orbitals and Organic Chemical Reactions", John Wiley & Sons, Inc., New York, NY, USA, (1976).

[28] Murray J.S., Sen K., "Molecular Electrostatic Potentials, "Volume 3, 1st ed., Concepts and Applications", Elsevier, Amsterdam, The Netherlands, (1996).

[29] Sponer J., Hobza P., DNA Base Amino Groups and Their Role in Molecular Interactions: *Ab Initio* and Preliminary Density Functional Theory Calculations, *International Journal of Quantum Chemistry*, **57**: 959-970 (1996).

[30] Johnson B.G., Gill P.M.W., Pople J.A., The Performance of a Family of Density Functional Methods, *J. Chem. Phys.*, **98**: 5612- (1993).

[31] Pople J.A., Scott A.P., Wong M.W., Radom L., Scaling Factors for Obtaining Fundamental Vibrational Frequencies and Zero-Point Energies from HF/6–31G* and MP2/6–31G* Harmonic Frequencies, *Isr. J. Chem.*, **33**: 345- (1993).

[32] Krishnakumar V., John Xavier R., Molecular and vibrational Structure of 2-Mercapto Pyrimidine and 2,4-diamino-6-hydroxy-5-nitroso Pyrimidine: FT-IR, FT-Raman and Quantum Chemical Calculations, *Spectrochimica Acta. Part A.*, **63**(2): 454-63 (2005).

[33] Socrates G., Infrared and Raman Characteristic Frequencies, 3rd ed., John Wiley & Sons Ltd., Chichester, (2001).

[34] Beraldo H., Barreto A.M., Vieira R.P., Rebolledo A.P., Speziali N.L., Pinheiro C.B., Chepuis G., Structural Studies and Spectral Characteristics of 4-Benzoylpyridine Thiosemicarbazone and N(4′)-phenyl-4-benzoylpyridine Thiosemicarbazone, *J. Mol. Struct.*, **645**: 213–220 (2003).

[35] Stuart B.H., Infrared Spectroscopy: Fundamentals and Applications, John Wiley & Sons, Inc., England, (2004).

[36] Chandra S., Saleem H., Sundaraganesan N., Sebastian S., The spectroscopic FT-IR Gas Phase, FT-IR, FT-Raman, Polarizabilities Analysis of Naphthoic Acid by Density Functional Methods, *Spectrochim. Acta A*, **74**: 704-713 (2009).

[37] Silverstein R.M., Webster F.X., "Spectroscopic Identification of Organic Compound", 6th ed., John Willey & Sons, Inc., New York, (1998).

[38] Pulay P., Fogarasi G., Pang F., and Boggs J.E., Systematic ab Initio Gradient Calculation of Molecular Geometries, Force Constants, and Dipole Moment Derivatives, *J. Am. Chem. Soc.*, **101**: 2550–2560 (1979).

[39] Chandran A., Varghese H.T., Mary Y.S., Panicker C.Y., Manojkumar T.K., Alsenoy C.V. Rajendran G., FT-IR, FT-Raman and Computational Study of (E)-N-carbamimidoyl -4- ((4-methoxybenzylidene)amino) benzenesulfonamide, *Spectrochim. Acta. A Mol Biomol Spectrosc.*, **92**:84-90 (2012).

[40] Gonohe N., Abe H., Mikami N. and Ito M., Two-Color Photoionization of van der Waals Complexes of Fluorobenzene and Hydrogen-Bonded Complexes of Phenol in Supersonic Jets, *J. Phys. Chem.*, **89**: 3642-3648 (1985).

[41] http://www.way2drug.com/PASSOnline/predict.php

[42] McConnell, Thomas H. (2007)."The Nature of Disease: Pathology for the Health Professions. Baltimore", Mar.: kLippincott Williams & Wilkins. p. 159. ISBN 978-0-7817-5317-3., Archived from the Original on 8 September (2017).

[43] http://www.swissdock.ch/docking

[44] https://www.rcsb.org/structure/5P4Q

[45] http://www.fao.org/docrep/x5348e/x5348e03.htm